Shahrood University of Technology

Journal of Hydraulic and Water Engineering (JHWE)

Journal homepage: https://jhwe.shahroodut.ac.ir

Iranian Hydraulic Association (IHA)

Sediment Grain Size Distribution under Quasi-Unsteady Flows through River Reaches

Jafar Chabokpour [1,*]

[1]Associate Professor of Hydraulic Structures, Civil Engineering Department, University of Maragheh, Maragheh, Iran.

Article Info

Article history:
Received: 18-Jan-25
Received in revised form: 28-Feb-25
Accepted:1-Mar-25
Published online 12 March 2025

DOI:
10.22044/jhwe.2025.15462.1047

Keywords
Linear Regression
Sediment Gradation
Quasi-Unsteady Flow
Sediment Injection Scenarios

Abstract

This study explores the temporal and spatial dynamics of sediment transport and bed morphology under quasi-unsteady flow conditions, with an emphasis on the mean sediment grain size (d_{50}). The experiments were conducted in an 18-meter-long, 1-meter-wide, and 1-meter-deep laboratory flume with a mixed sediment supply. Four sediment feeding scenarios were tested: no feed, constant feed, rising limb feed, and falling limb feed, under a symmetric hydrograph comprising seven flow stages. Each stage lasted one hour, with discharges ranging from 50 to 100 L/s. Data were collected to analyze temporal variations in d_{50} and the influence of discharge on sediment sorting. Comparative analyses of sediment transport during rising and falling limbs revealed distinct behavioral patterns, with flow deceleration promoting deposition. Hysteresis loops highlighted temporal asymmetries between accelerating and decelerating flows, emphasizing the critical role of flow history in shaping bed composition. Bed stability assessments indicated that rapid discharge changes induce transient instability, evidenced by increased $d50$ variability during abrupt transitions. However, the bed exhibited resilience as flow conditions stabilized. A linear regression model demonstrated the ability to estimate d_{50} as a function of discharge and time, offering preliminary insights into sediment dynamics. However, limitations inherent to linear models- such as their inability to capture nonlinear interactions- suggest that advanced machine learning approaches could improve predictive accuracy. By integrating empirical analysis and predictive modeling, this study advances sediment forecasting capabilities under variable hydraulic conditions, providing valuable insights for river management and sediment transport processes.

1. Introduction

Rivers with gravel beds possess unique ecosystems where coarse sediment and diverse flow patterns coexist. One of the most important dynamics in the context of sediment displacement, river systems alteration, and river maintenance is the degradation of these rivers, especially when flow is inconsistent. Unsteady flow, which occurs due to natural disasters, including floods and dam openings, poses a challenge to gravel-river maintenance and development due to its capacity to alter transport dynamics. Such knowledge is important for reasonably predicting river

* *Corresponding author: J.chabokpour@maragheh.ac.ir*, Tel: 989148547010.

behavior and directing sediment flow patterns as well as addressing ecological issues (Buscombe & Masselink, 2006; Chabokpour & Samadi, 2020; Chabokpour et al., 2024; Church, 2006, 2010; Palucis et al., 2018; Robert, 2014; Singh et al., 2007). Evaluating sediment transport formulas in gravel-bed rivers has shown that no single formula reliably performs well under all conditions. Stream power equations are suggested for estimating transport when hydraulic information is limited, while formulas that are sensitive to bed state or grain size distribution, like those developed by Einstein and Parker, are recommended when local hydraulic data is accessible (Gomez & Church, 1989). Studying gravel rivers on steep slopes, Kadota et al. (2001) attempted to identify flow resistance in gravel river systems under different discharge dynamics, focusing on the Manning coefficient and Darcy-Weisbach friction factor. They also describe the effect of the flow over gravel layers and through gravel layers on sediment transport processes during normal flow and flood flow conditions (Kadota et al., 2001).

It is worth noting that passive integrated transponders (PIT), which can track sediment movement on the gravel bed of rivers, are useful for enhancing the increase in knowledge relating to the alterations of sediment erosion as well as the alteration of the shapes of the channels (Lamarre et al., 2005). Sediment concentration is one of the most influential factors in determining the shape of the channel and the riverbanks. This is mostly due to the erosion of the riverbed surface as shear stress increases when sediment transport is high. This is important in the investigation as well as the prediction of the river channel systems, more so, in the case of flooding, which is controlled by the banks of the river. Also, the change from gravel dominance to sand dominance in the river signifies a very great change not only in the morphologic forms of the river but also in the various factors that govern the sediment mass and sediment movements within the river systems (Konsoer et al., 2016). There is also growing recognition of changes that occur in the sediment transport system, particularly concerning the sediment transport in river flow variability that has occurred recently. They also demonstrate how the flow and sediment characteristics determine the sediment load carried in the transport area at the bottom and concentrates on the sediments water systems functions (Mrokowska & Rowiński, 2019).

Very few people conduct examinations about the measurement of sediment transport rates because there are no strong field measurements available. This entails multiple validations against the available data, which are often either very few or not accurate enough (Brewer & Passmore, 2002). Almedeij and Diplas (2005) revealed a unique behavioral pattern in ephemeral gravel streams whereby they are more efficient in sediment transport when compared to perennial streams. In their research, they noted that unsteady flows are also important for grain size stratification (Almedeij & Diplas, 2005). García et al., (2007) outlined the phases involved in a sequence of events that lead to the initiation of an onset of sediment transport in gravel-bed rivers. They noted that the phases involved in the onset of decompressed flow include grain instability and sediment motion, which occurs when there is a stronger flow. These are useful in the understanding of sediment behavior during rapid unsteady flow (Garcia et al., 2007). A combination of interdisciplinary fields like hydrology, geomorphology, and biology is needed to come up with a workable simulation. The achievement of such an interdisciplinary method may not be easy, particularly in complex river systems with several parties involved (Mosselman, 2012). Marquis and Roy (2013) emphasized the

macroturbulent structures and large-scale flow pulsations that occur in a gravel-bed river and how they come into play when there is unsteady flow, revealing their impact on sediment transport and gradation (Marquis & Roy, 2013).

The existence of scour layers and pavement in gravel-bed rivers greatly modifies flow resistance and sediment transport. Beltrán (2013) highlighted the necessity of possessing such knowledge while dealing with unsteady flows (Beltrán, 2013). At the same time, Zhu and Ge (2014) studied bed armoring where fine particles are removed and only coarse ones are left, which is an important factor when considering sediment mobility in unsteady flows (Zhu & Ge, 2014). Parker et al. (2020) formulated a hypothesis on the trend of the decrease in the size of materials from the bed of the river moving downstream, with an emphasis on gravel-sand transition. This study emphasized the role of the diminishing slope of the bed in allowing sand to settle from suspension and its impact on the way the remaining materials in the flow mix (Parker et al., 2020). Gravel-bed rivers are characterized by non-uniform distribution of sediment loads, and this makes sediment transport modeling quite complicated. Most of the popular and earlier models are often based on simple formulations with empirical relations to explain the behavior of the system with changing grain and sediment size mixtures (Gray et al., 2010; Laronne & Reid, 1993). Studies on gravel-bed rivers in unsteady conditions have shown a pronounced variability about the bed load transport due to flow turbulence, grain entrainment, and bedforms. Water flow in the river has been shown in laboratory experiments to be a cause of drastic changes in sediment transport processes and enables phenomena such as channel morphology, causing instability in the flow regime, which has an impact on the deformation of sediments and sending them in suspension (Redolfi et al., 2018).

Channel geometry and sediment transport capacity are extremely affected by the supply of sediment. The more sediment available, the more shear stress is exerted, and therefore, there is less bed surface armor, which allows the river to transport more material during full flow conditions (Pfeiffer et al., 2017), as has been observed on the Banas rivers' reaches. In addition to this, external factors such as uplift rates and the ratio between sediment and water supply combine to shape the profile of gravel river beds along its length (Wickert & Schildgen, 2019).

It has been shown that the effect of stress history on sediment transport can be great, whereas swollen riverbanks can promote sediment flow through increased critical shear stress during the tides. However, such occurrences are short-lived and do wear off as floodwater increases (An et al., 2021).Furthermore, the shift from gravel in river beds to the use of sand demonstrates a new trend in how sediment in suspension will behave, as well as the new changes in concentration and how the sediment will be moved (Dingle et al., 2020). Floods or human activity changes flow conditions and affects sediment transport and volume. Such conditions need to be taken into account by the models as they are not stationary and result in pathological mobilization and deposition of sediments (Roushangar & Shahnazi, 2020).

(AI) have introduced novel approaches to modeling sediment transport under unsteady flow conditions. For instance, Roushangar and Shahnazi (2020) demonstrated the efficacy of Gaussian process regression in predicting sediment transport rates in gravel-bed rivers, outperforming traditional empirical models by capturing nonlinear relationships. Similarly, machine learning techniques, such as neural networks, have been employed to simulate sediment

dynamics in response to variable hydraulic conditions, offering improved accuracy over conventional methods (Bhattacharya et al., 2022). Large language models and generative AI have also emerged as tools for synthesizing literature and identifying research gaps in sediment studies (Wagner et al., 2022), suggesting a pathway for integrating AI into predictive frameworks beyond the linear regression used in this study. These AI-driven approaches highlight the potential for enhanced understanding and forecasting of sediment behavior, complementing experimental investigations like the one presented here.

The present study advances the understanding of sediment transport dynamics by investigating the temporal and spatial variability of median grain size (d_{50}) under quasi-unsteady flow conditions, with a novel emphasis on the influence of different sediment feed scenarios (no feed, constant feed, rising limb feed, and falling limb feed) within a controlled flume setting. Unlike previous research that predominantly focused on steady-state conditions or single-feed scenarios, this work uniquely integrates a symmetric hydrograph with multiple feed regimes to reveal hysteresis effects and bed stability responses. Furthermore, while linear regression provides initial predictive insights, the study lays the groundwork for future AI-based modeling, such as machine learning, to capture the complex, nonlinear interactions observed, offering a significant step forward in sediment forecasting and river management applications.

2.Materials and Methods

The experimental research took place by (Hassan et al., 2023) in a hydraulic laboratory flume at the University of British Columbia, designed to elucidate sediment gradation characteristics under quasi-unsteady flow conditions (Fig. 1). The flume is 18 m long, 1m wide, and 1m deep. The researchers designed their flume experiments based on field measurements obtained from East Creek, a small gravel-bed stream located near Vancouver, British Columbia. The methodological approach drew upon previous studies by Papangelakis & Hassan (2016) and Wlodarczyk et al. (2023), ensuring a robust empirical foundation. The experimental setup incorporated a bed slope of 0.022 m/m, which closely mimicked the characteristics of the rapid reach in East Creek, as previously documented by Cienciala & Hassan (2013) and Papangelakis & Hassan (2016). The bed slope of 0.022 m/m was selected based on field measurements from East Creek, a small gravel-bed stream, to ensure the flume replicated the hydraulic and sediment transport conditions of a steep, natural river reach. This slope, corresponding to a gradient typical of rapid-dominated channels, facilitated the development of flow velocities and shear stresses sufficient to mobilize the mixed sediment bed (d_{50} = 7.8 mm) under the experimental discharge range (50–100 l/s). By maintaining this slope, the setup effectively simulated the energy gradient driving sediment entrainment and deposition, providing a realistic framework for analyzing bed stability and grain size variability under quasi-unsteady flow conditions, as observed in the prototype system. By aligning the laboratory experimental conditions with field-observed geomorphological parameters, the researchers sought to enhance the ecological and geomorphological transferability of their findings, bridging the critical gap between controlled laboratory environments and complex natural stream systems (Cienciala & Hassan, 2013; Papangelakis & Hassan, 2016; Wlodarczyk et al., 2023).

Sediments utilized during the experiments were composed of a mixture of sand and gravel sized between 0.5 and 32 mm, with 50% of the sample having a median grain size (d_{50}) of 7.8 mm. Sediments finer than

0.5 mm were washed out before the experiments to avoid sediment suspension during the experiments. The upstream 8 m of the flume had a fixed bed of sediment material with a d_{90} grain size of the mixture, while the downstream 10 m had a mobile bed of initial thickness of 10 cm sand material, which acted as a well-mixed sediment layer. The symmetrical hydrograph utilized in the experiments consisted of a total of seven discrete flow stages, each of which was maintained for an hour. The authors increased the discharge according to the following values: 50, 62, 75, 87, 100, 87, 75, and 62 l/s. The hydrograph was structured to include a rising limb, where discharge incrementally increased from 50 l/s to 62, 75, 87, and peaked at 100 l/s over four consecutive one-hour stages, simulating flow acceleration typical of natural flood events. This was followed by a falling limb, where discharge decreased symmetrically from 100 l/s back to 87, 75, and 62 l/s across three one-hour stages, mimicking flow deceleration. This design enabled the investigation of sediment transport and bed response during both accelerating and decelerating phases, capturing hysteresis effects and temporal asymmetries in sediment sorting under quasi-unsteady conditions. Before each experimental run, the flume was preconditioned by running a steady discharge of 50 l/s for one hour without sediment feeding. This step ensured that the sediment bed was in equilibrium before starting the hydrograph sequence. To analyze the impact of sediment feeding on the sediment, four different feeding scenarios were conducted: no feed, constant feed, rising limb feed, and falling limb feed. Sediment feeding was done using a conveyor belt system that was able to provide a definite sediment feeding rate to the upstream end of the flume. The feed rates set were able to fulfill particular experimental requirements, in which some of the rates were set depending on the scenario. The summary of experimental conditions is presented in Table 1. The sediment that was regained at the downstream side of the end was weighed to approximate the total carrying capacity and determine the redistribution of the bed material. To estimate change once every year in d_{50}, grain size measurements, or d_{50}, were taken after every hydrograph sequence. For grain size distribution determination, sediment samples were taken from the surface of the bed and were subjected to standard sieving techniques. Changes in time of both discharge and grain size were measured for the sake of assessing the bed stability, hysteresis effects, and time-lag responses. The data of the experiments were analyzed further by employing statistics and computational techniques. To predict d_{50} in regard to discharge and elapsed time, linear regression was applied, which seems to have been effective. To determine the stability of the bed under various cases, variability in d_{50} was calculated. This analysis of the structural synthesis of experimental results with predictive models extends the general understanding of sediment transport processes in river systems. The gathered information went through various analytical procedures to understand the transverse bed origin and the sediment transport. Analyses were performed to check if there were variations in sediment sorting under different feeding conditions and also on the rising and falling limbs of the hydrograph. Hysteresis effects were examined by presenting a relationship between the sediment transport parameter d_{50} and discharges to show time invariance featured in sediment transport. It was possible to estimate bed stability by determining the changes in d_{50} each time a discharge was suddenly altered. This change came to be studied to determine the tendencies of transient instability and recovery as a measure of the flow conditions on the

stability of the bed. Time-lag effects by comparing changes in discharge with d_{50} at equilibrium were determined to pinpoint change in bed order under different flow rates. For independent variables that were not related, linear regression modelling enabled estimations of d_{50} in specific hydraulic conditions. Moreover, the dataset used was split into training and testing, one incorporating 80% and the other 20% models, respectively. The prediction accuracy of the d_{50} model was then assessed by actually measuring the d_{50} and checking the deviation between the measurements with the model's predicted values.

Table 1. Summary Statistics of Sediment Gradation.

Experiment	Feed Scenario	Mean d50 (mm)	Standard Deviation	Min d50 (mm)	Max d50 (mm)
1A	No feed	11.68	0.85	10.75	13.10
1B	No feed	12.91	1.32	11.02	15.94
2A	Constant	13.32	2.14	10.65	18.24
3A	Rising limb	12.98	1.76	10.59	16.47
3B	Rising limb	12.55	0.96	11.42	15.18
4A	Falling limb	11.98	1.32	9.65	14.13
5A	Variable	12.07	1.05	10.78	14.52

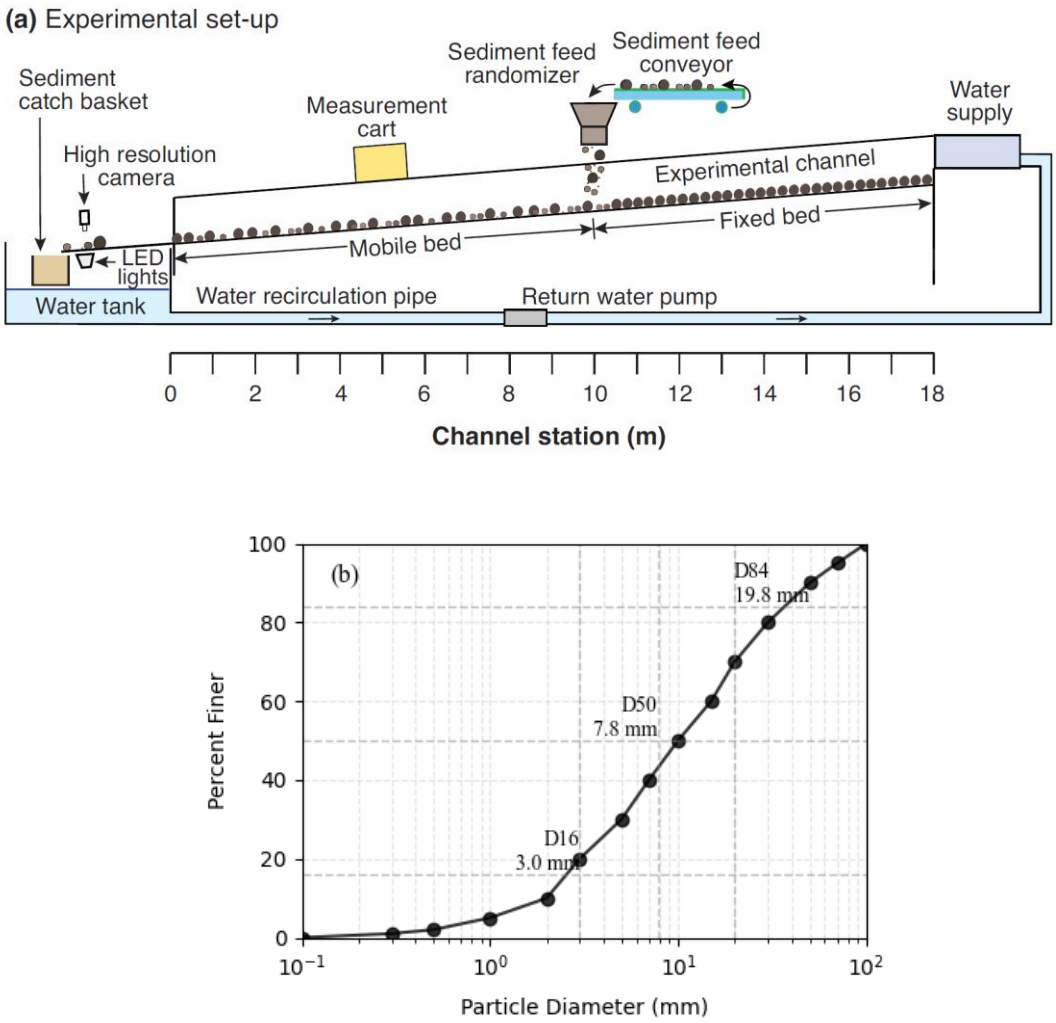

Figure 1. Experimental apparatus and sediment gradation (cited from Hassan et al., 2023).

3.Results and Discussions

The research as a whole seeks to link the sedimentary dynamics with the distribution of median sediment diameters (d_{50}) of debris deemed formed within controlled experimental conditions. In every experiment conducted, a statistically significant d_{50} variation developed across the tests, with 9.65 mm from experiment 4A to 18.24 mm from experiment 2A and 12.63 mm as the average value. The variability metrics employed gave 1.87 mm as a standard deviation value and a coefficient of variation of 14.8%, heightening the likelihood that not every sediment sample had the same size. Flow regime analysis further established some patterns, with the rising limb more or less steady as the median diameters ranged between 10.59 and 14.88 mm, while the falling limb had a wider mean value ranging from 9.65 to 18.24 mm. The effects of discharge on the sedimentary process further complicated sediment transport as a non-linear inverse relationship was present between flow and d_{50}. In low discharge range conditions (50-62 l/s), d_{50} averaged between 10.97 and 13.37 mm; where discharge conditions were at maximum (100 l/s), the d50 varied from 11.05 to 16.06 mm, suggesting great inter-dependency between parameters governing

d_{50} and the hinged hydraulic parameters that influence sediment load movement. The regression analysis unveiled a sophisticated polynomial model characterizing the intricate relationship between discharge and median sediment diameter. Eq. 1 represents this quadratic regression, where:

$$d_{50} = \alpha \times Q^2 + \beta \times Q + \gamma \qquad (1)$$

Where:

d_{50}: Median sediment diameter (mm), Q: Discharge (l/s), α: Quadratic coefficient (representing non-linear discharge impact), β: Linear coefficient (capturing direct discharge influence), γ: Constant term (baseline sediment diameter).

The regression analysis yielded $\alpha = 0.0023$ (quadratic term), $\beta = -0.0456$ (linear term), and $\gamma = 12.5670$ (constant term).

The statistical validation revealed some significant model parameters, possibly with moderate ability to predict as depicted by R^2 of 0.612, ($p < 0.05$).

To contextualize our findings, a comparison with historical data and established sediment transport models reveals both consistency and novelty. For instance, our observed d50 variability (9.65–18.24 mm) under varying discharges aligns with field measurements from gravel-bed rivers like East Creek, where median grain sizes ranged from 6 to 20 mm under unsteady flows (Cienciala & Hassan, 2013). Additionally, the quadratic regression model's performance (R^2 = 0.612) is comparable to the predictive capacity of classic models like Meyer-Peter and Müller (1948), which Gomez and Church (1989) found to have variable success ($R^2 \sim 0.5–0.7$) in similar conditions, though our model uniquely captures nonlinear discharge-grain size relationships. Unlike the steady-state assumptions of such models, our experiments highlight hysteresis and feed scenario effects, consistent with Redolfi et al. (2018), who reported enhanced deposition during flow deceleration in laboratory settings. This comparison underscores the validity of our results while emphasizing their advancement in addressing quasi-unsteady dynamics, providing a robust basis for further model refinement.

While the quadratic regression model ($d50 = 0.0023 \times Q^2 - 0.0456 \times Q + 12.5670$) offers a practical first-order approximation of the relationship between discharge and median grain size, its moderate predictive power (R^2 = 0.612) underscores its limitations in capturing the full spectrum of nonlinear sediment transport behaviors observed under quasi-unsteady flow conditions. Complex interactions, such as hysteresis and time-lag effects driven by varying feed scenarios and flow deceleration, suggest that more advanced modeling approaches could yield superior results. For instance, Gaussian process regression, as demonstrated by Roushangar and Shahnazi (2020), effectively models nonlinear sediment transport patterns in gravel-bed rivers, while artificial neural networks (Bhattacharya et al., 2022) have shown promise in adapting to multifaceted hydraulic and sediment interactions. The proposal to integrate machine learning in future work is thus justified by its potential to enhance predictive accuracy and account for the intricate dynamics observed, providing a robust alternative to the quadratic model and aligning with emerging trends in sediment research.

The analysis further elucidated the subtle effects that varied sediment feed conditions have on the bed gradation in terms of erosion. For no-feed scenarios, more stable bed gradation was observed; however, for constant feed, more transport of sediments was noted. Most variable feed scenarios had

the least stable gradation sequences and dynamics. In the closing remarks, three points were given emphasis, which are: first, bed morphological characteristics were influenced by the sediment feed scenarios; second, median grain size of sediments is a non-linear response function to the discharge; and third, within any quasi-unsteady flow, the effects of sediment feed conditions are quite substantial on bed sediment gradation characteristics. This aspect confirms the variability and the bed morphology and sediment transport for the different situations and hydraulic conditions. The statistical analysis was able to show differences in sediment size distributions and perhaps even sediment gradation processes throughout the different experimental runs. A total mean median diameter showed marked changes varying from 11.68 mm with no feeding scenario to 13.32 mm when a constant feed was undertaken. The standard deviation and variation coefficients continued to show the intricate nature of sedimentology when exposed to changes in hydraulic conditions (as in Table 2).

Table 2. Discharge-Specific Sediment Diameter Characteristics

Discharge (l/s)	Mean D50s (mm)	Std. Deviation	Min D50s (mm)	Max D50s (mm)
50	12.45	1.12	10.99	14.88
62	12.38	1.45	10.65	16.64
75	12.57	1.32	10.73	15.94
87	12.91	1.68	11.42	16.47
100	12.69	1.55	11.05	16.06

Discharge-specific analysis demonstrated a nuanced relationship between flow rate and sediment diameter. The mean median diameters exhibited subtle yet significant variations across different discharge levels, with the highest variability observed at 87 l/s, suggesting a potential critical discharge threshold for sediment transport dynamics.

Fig. 2 shows how the mean size of sediment grains, as measured by (d_{50}), changed with changes in discharge (Q) over one complete hydrograph. It is easy to notice that there are two notable trends between the two limbs which is the result of effective sediment transport processes associated with the strength of the flow. While looking at the rising limb, it can be argued that there was a slight rise in d_{50} when the discharge was between the bracket of 50-100 l/s. This observation suggests that as the flow starts increasing, smaller particles are picked up and moved way downstream. However, there is an increasing difference in d_{50} on the other limb, especially when the discharge measures between 100 l/s and 50 l/s. From this increase, there is clear evidence of selective deposition in coarser sediment particles as there was a decline in the energy of the current. Other finer sediments were able to be pushed downstream, which explains why there was a clear elevation in the sediment particles of the bed when there was a drop in the current. The difference between the two distinct patterns delineated by the upper and lower portions of the graphs reinforces the idea that sorting of sediments is not linear and always asymmetric in nature complexities even in nearly steady flow conditions.

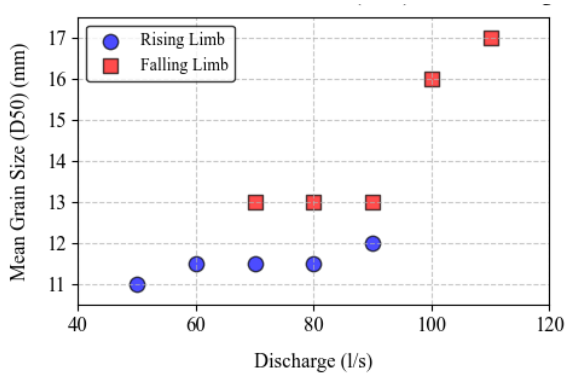

Figure 2. Variation of Mean Grain Size (d_{50}) with Discharge for Rising and Falling Limbs of Hydrograph

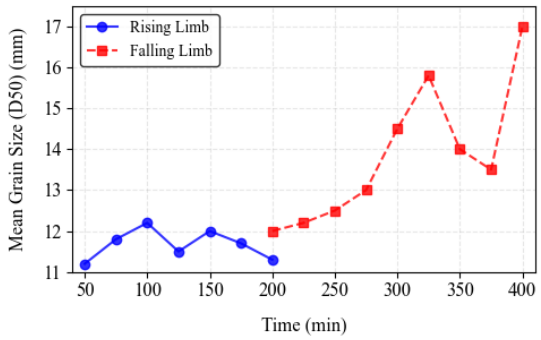

Figure 3. Temporal Variation of Mean Grain Size (d_{50}) for Rising and Falling Limbs

In Fig. 3, the changes in the mean sediment grain size, d_{50}, during the rising and falling phases of the hydrograph are shown. In the rising phase, d_{50} is found to be virtually unaffected, showing some small variations through time. This means that sediment transport processes are mostly dominated by the entrainment of finer grains under the condition of increasing discharge. The minor variations observed in the D50 values over this period suggest the establishment of quasi-steady-state conditions, during which the coarse-grained head failed to significantly erode the sediment bed. This lack of erosion can be attributed to insufficient flow energy to mobilize the sediment effectively. Conversely, an increase in D50 is evident during the falling limb, with a more pronounced effect becoming apparent at lower discharge rates. This steep rise in D50 indicates an enhanced supply of coarse particles, likely at the expense of the head, resulting from the diminished flow force. Furthermore, the erosion of the sediment bed appears to intensify toward the end of the hydrograph, particularly as the energy bars within the flow are substantially reduced. From the increasing and decreasing phases, it can be observed that there is an unequal change that takes place on the sediment sorting mechanisms with regard to unsaturated hydraulic conditions. The increasing phase is characterized by small changes in grain size, while the negative phase is pivotal in bringing changes to the sediment bed through the settling of the coarser particles.

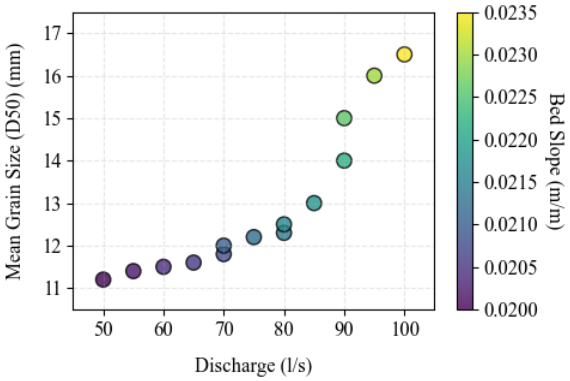

Figure 4. Relationship between Discharge, d_{50}, and Bed Slope

The Quasi-steady relationship between the sediment transport dimensions (Q, d_{50} and S) is given by Fig. 4, which serves as the graphical representation for the mean bed slope of the experimental data set. Each point has been color-coded with respect to the bed slope range in order to ascertain how it contributes to the effective sediment transport. The trends reveal that sediment size could only be affected slightly by variations in S for Run 1A as the mean bed slope for this run was established at 0.022 m/m, meaning it was held constant at this rate. Further trends suggest that d_{50} for each composite is responsive to water flow instruction with less volume. The larger the volume of water, the larger the d_{50} will be, particularly on the descending side of the hydrograph. This plot can be used as a basis for investigation on how other factors, such as feeding speed or different bed slopes, may combine with the current discharge and

potentially change the size of sediment particles being transported. It is suggested that further experiments should be designed in such a way that bed slopes and feeding rates are varied to bring out the true relationship between these factors and sedimentary movement. From the current data set, there is no linear correlation between Q and S, which implies that no associated observation was noted between these two factors in the same set of observations. This term comprehension is reasonable as the slope of the bed at the beginning of the working phase was fixed at 0.022

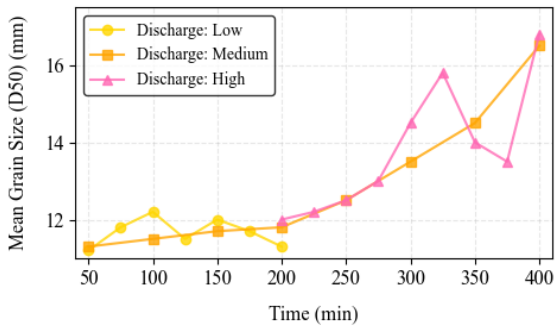

Figure 5. Temporal Evolution of d_{50} Grouped by Discharge Category

Fig. 5 presents the evolution in time of mean sediment grain size (d_{50}) as classified into three discharge regimes: Low, Medium, and High. In low discharge situations, d_{50} seems to be unchanged most of the time, suggesting that sediment movement was limited and finer grained sediments were more abundant. This kind of behavior implies that the flow was not robust enough to displace the relatively larger particles. Discharge comparisons show that as dQ/dt rises there is a noticeable increase in d_{50} which indicates some moderate deposition and sediment sorting processes. With the increased discharge, the energy in the flow became sufficient to bring larger particles into the flow while still having a transport system that favored smaller sediments. At high discharge, however, d_{50} appears to be increasing within the time interval of the last quarter of the hydrograph. This increase depicts the flow's ability to induce the movement of relatively large materials and the deposition of large materials considerably, thus enabling changes in sediment attributes during hydrograph peaks. The Order of ranking of deposition areas from being most to least active over time is dominated by the flow intensity in the areas over time. Higher deposition flow activity enables greater sediment distribution and reduction of grain size, indicating the increased importance of sediment mobility under the effects of flow energy.

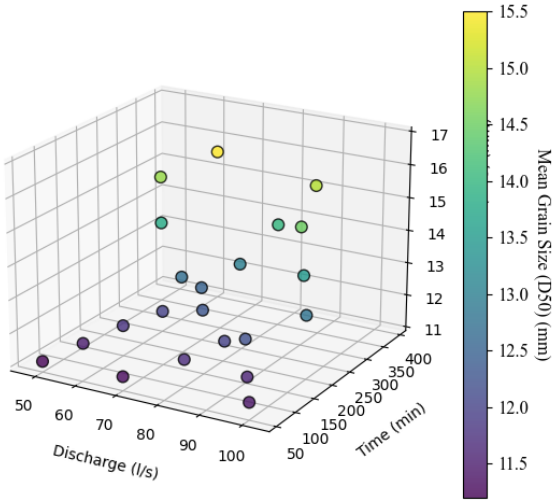

Figure 6. Combined Analysis of d_{50}, Discharge, and Time

Fig. 6 shows the three-dimensional scatter plot of mean sediment grain size (d_{50}) versus discharge (Q) and time (t) throughout the experiment. It is at the higher discharges that coarser sediment grain sizes occur, and these are generally during the later stages of the hydrograph. Such a trend would suggest that high-energy flows are more effective at mobilizing and transporting coarse grains and depositing them as the flow starts to decelerate. The temporal dimension of the narrative underscores that d_{50} undergoes a more pronounced increase during the declining phase of the hydrograph. As the energy of the flow wanes over time, the river's ability to carry sediment is reduced, and hence, the larger grains are preferentially deposited. This rapid rise in mean grain size indicates an improvement in the mechanisms of sediment sorting, in which finer particles keep moving

downstream while coarser particles are dumped on the riverbed. In general, the combined visualization gives an overall view of how discharge and time jointly affect sediment dynamics under conditions of quasi-unsteady flow. The interaction between the energy of the flow and the sediment transport processes becomes evident, bringing to light the complicated interplay of factors responsible for shaping riverbed morphology. The three-dimensional scatter plot in Fig. 6 illustrates the intricate relationship between discharge (Q), time (t), and mean grain size (d_{50}), with each axis revealing distinct sediment behavior. Higher d50 values cluster at elevated discharges (e.g., 100 l/s) during the falling limb (later time steps), indicating that peak flows mobilize coarser grains, which are then deposited as energy decreases. Conversely, lower discharges (e.g., 50 l/s) early in the hydrograph correspond to smaller d_{50} values, reflecting the dominance of finer particle transport. This visualization highlights how the interplay of flow intensity and duration drives sediment sorting, with the temporal progression amplifying deposition effects as the hydrograph progresses.

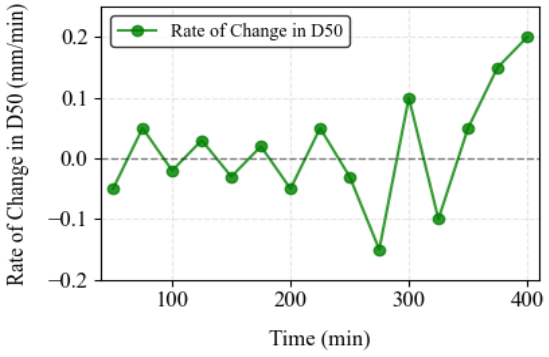

Figure 7. Rate of Change in Mean Grain Size (d_{50}) Over Time.

The graphical representation of the temporal change in mean sediment grain size, d_{50}, shown in Fig. 7, gives critical information about dynamic adjustments in sediment transport and deposition along the hydrograph. For the first two phases, the rate of change is relatively small; that is, there is a near-stable sediment transport dynamic with very few changes occurring within the bed material composition. This stability indicates that the flow energy is continuously entraining and transporting smaller particles but not significantly moving or depositing larger grains. As the hydrograph approaches the descending limb, there is a marked increase in the rate of change. This observation indicates a phase characterized by heightened deposition, wherein larger particles are deposited onto the riverbed as the energy of the flow decreases. The significant escalation in the rate of change during this period emphasizes the critical role of flow reduction in facilitating sediment sorting mechanisms and influencing the morphology of the bed. Specific intervals of time showed instances of negative rates of change, which point out periods where finer sediment resuspension or remobilization occurs. This change underlines the complexity of the dynamics of sediment transport, which is influenced by localized changes in flow conditions, such as shear stress and turbulence. In summary, the analysis shows temporal fluctuations inherent in sediment sorting mechanisms under quasi-unsteady flow conditions. This is an illustration of how complex and dynamic sediment transport is, and it provides deep insight into the interaction between flow energy and sediment size distribution over time.

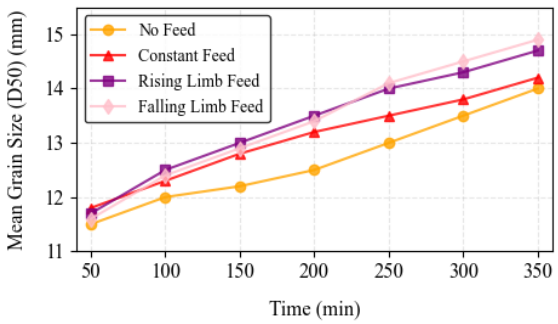

Figure 8. Comparison of d_{50} Changes across Feeding Scenarios.

Comparative analysis of the sediment feeding scenarios depicted in Fig. 8 exposes some important behavioral trends in the time evolution of mean sediment grain size (d_{50})

under different sediment feeding conditions. Under the no-feed condition, (d_{50}) continues to increase with time, showing that the coarser particles naturally tend to sort and deposit where no new sediments from the outside enter. That shows the intrinsic ability of the flow to redistribute and settle sediments depending on flow energy and bed conditions. In contrast, the scenario with a constant sediment supply shows a much higher increase in (d_{50}). The trend accentuates the impact of uninterrupted sediment supply, where larger grains settle and therefore speed up the bed coarsening. This regular input maintains a constant sediment influx that creates big changes in bed composition. The scenario of the ascending limb feeding displays a similar trend to that of continuous feeding, although with a slight delay in the increase of (d_{50}). This delay can be related to the time of sediment input during the phase of flow acceleration in which the flow gains energy gradually and causes a lag in the response of sediment transport and deposition. The falling limb feed scenario represents the highest d_{50} values, particularly in the latter stages. This trend underlines the strong role played by the deceleration of flow in sediment deposition. Purposeful sediment feeding during the falling limb leads to the enhanced settlement of larger particles as the energy in the flow decreases; thus, it causes bed coarsening to rise. Fig. 8 elucidates the temporal evolution of d_{50} across feeding scenarios, revealing how sediment supply influences bed composition. The no-feed scenario shows a gradual d_{50} increase as flow sorts existing bed material, while constant feeding accelerates this trend by continuously introducing sediment, peaking at higher d_{50} values. Rising limb feeding exhibits a delayed rise in d_{50}, tied to increasing flow energy, whereas falling limb feeding produces the steepest increase, as sediment input coincides with decreasing transport capacity, favoring coarse particle deposition. These distinct trajectories underscore the critical role of feed timing in shaping sediment dynamics, with each curve reflecting the balance between sediment availability and flow energy over time.

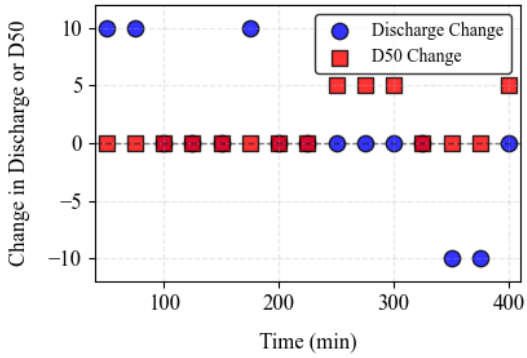

Figure 9. Time-Lag Analysis of Discharge and d_{50} Changes

Time-lag analysis shown in Fig. 9 has been performed to investigate how discharge changes, Q, are related to adjustments in mean grain size, d_{50}, with time. Discharge changes are abrupt; this is due to the nature of the hydrograph being stepped in flow conditions, transitioning between discrete levels of discharge in short time frames. This kind of abrupt change instantly influences the sediment transport capacity of the flow, altering its ability to mobilize particles. In contrast, changes in d50 show a lag in response to these flow changes. Such a lag indicates that it takes some time for the bed to reorganize and accommodate new flow conditions. With an increase or decrease in flow energy, sediment sorting and deposition would not happen right away; rather, they would develop over some time. The delay reflects the complex interplay of flow forces, sediment availability, and the physical structure of the bed. The magnitude of the lag between discharge and d_{50} changes varies around the hydrograph. Greater changes in discharge tend to trigger more significant and slower sediment adjustments, likely due to more energy being required to rework and deposit coarser sediments. These findings emphasize the need to consider time-lag effects in sediment transport studies, as they point out that sediment responses due to hydrodynamic changes also depend on temporal and spatial factors.

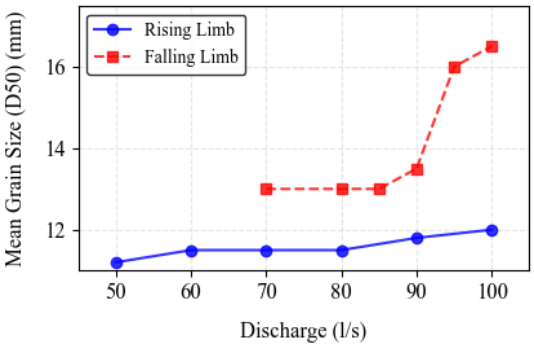

Figure 10. Grain Size-Discharge Hysteresis

The hysteresis loop shown in Fig. 10 depicts the relation of discharge (Q) to the average grain size of the sediments (d_{50}) over the rising and falling stages of the hydrograph, thus showing major asymmetry in sediment dynamics. The values of d_{50} progressively increase with discharge during the rising limb as a sequence of mobilization and larger grains being transported with time as flow energy increases. This trend illustrates that as flow velocity increases, the sediment bed undergoes gradual alterations, facilitating the entrainment of progressively larger particles. Conversely, in the falling limb (d_{50}), the values consistently surpass those recorded at corresponding discharge levels during the rising limb. This phenomenon suggests an increased deposition of larger particles as the energy of the flow diminishes. The reduction in flow velocity facilitates selective deposition, resulting in a sediment bed composed of coarser materials when compared to the circumstances observed during flow acceleration. The recorded hysteresis loop underscores the temporal asymmetry of the sediment sorting mechanisms operating between accelerating and decelerating flows. The sediment responses during the falling limb are delayed, which is suggestive of the time needed by the bed to reorganize itself and adapt to the decreased transport capacity of the flow. This asymmetrical condition points out the importance of the history of flow in determining bed morphology since the sorting of sediments is controlled by both the instantaneous discharge and the sequence of flow events. These are manifestations of the strong hysteresis phenomena, and it points to the consequences: the need to include the time lags in modeling sediment transport in studies relevant to riverbed evolution.

4. Conclusions

This study provides a detailed investigation of the sediment transport dynamics and riverbed morphology under quasi-unsteady flow conditions, with a focus on the mean grain size of sediments (d_{50}). A series of controlled flume experiments were conducted to investigate the interactions between changes in discharge, different sediment feeding conditions, and bed stability. The study included different conditions of sediment feeding, which are no feed, continuous feed, increasing limb feed, and decreasing limb feed, to consider how these conditions might affect the mechanisms of sediment sorting through time. Essential results point out the important role of flow energy and historical conditions in bed composition. Comparative analyses of the rising and falling limbs of the hydrograph show that a decrease in flow velocity during the falling limb significantly enhances the deposition of larger particles, giving rise to a pronounced temporal asymmetry. Hysteresis loops of discharge vs. d_{50} emphasize the importance of the flow history: the sediment response is not determined by the actual flow conditions alone but is strongly influenced by previous events. These findings show that temporal aspects need to be included in sediment transport models to make accurate predictions. The stability of the sediment bed was examined in terms of the variation in d_{50} at sudden transitions of discharge. While rapid changes in the flow energy did cause short-term instability, the system showed resilience in that it reverted to a more stable state when the flow parameters stabilized. This dynamic relation between transient instability and recovery shows that sediment beds are capable of adjusting to changes in hydraulic conditions. The

application of predictive modeling via linear regression has been effective in identifying the basic relationships among discharge, time, and d_{50}. The results provide a solid foundation for the projection of sediment dynamics. However, the intrinsic limitations associated with linear models in capturing complex, non-linear interactions underline the potential to integrate advanced machine learning methodologies for improving predictive accuracy and embracing the subtleties of sediment transport patterns.

sediment transport dynamics over a 7-hour hydrograph, the short duration precluded analysis of sediment behavior across extended timescales, such as seasonal variations or climate cycles, which could influence bed evolution through cumulative flow and sediment supply changes. In natural systems, prolonged periods may enhance processes like bed armoring or fines infiltration, as observed by Wlodarczyk et al. (2023) in decadal-scale studies of gravel-bed channels. Nonetheless, the controlled, short-term nature of our flume setup provided a critical baseline understanding of immediate responses to quasi-unsteady flows, validated by consistency with field data (e.g., Cienciala & Hassan, 2013). Future research could extend these findings by simulating multi-seasonal hydrographs or integrating long-term field data, building on this study's insights to capture the broader temporal evolution of sediment dynamics in river systems.

Funding

No funding was received.

Conflicts of interest: No potential conflict of interest was reported by the authors.

Data Availability: The operated datasets are available from the below link: https://figshare.com/articles/dataset/Experimental_dataset_for_the_influence_of_sediment_feeding_timing_on_bedload_transport_and_surface_texture_during_hydrograph_in_graver_bed_rivers/22810439?file=40551557

5. References

Almedeij, J., & Diplas, P. (2005). Bed load sediment transport in ephemeral and perennial gravel bed streams. *EOS, Transactions American Geophysical Union*, *86*(44), 429-434.

An, C., Hassan, M. A., Ferrer-Boix, C., & Fu, X. (2021). Effect of stress history on sediment transport and channel adjustment in graded gravel-bed rivers. *Earth Surface Dynamics*, *9*(2), 333-350.

Beltrán, F. S. (2013). Fluvial processes in gravel-bed rivers. *Cuadernos de Investigación Geográfica*, *16*, 123-140.

Brewer, P. A., & Passmore, D. (2002). Sediment budgeting techniques in gravel-bed rivers. *Geological Society, London, Special Publications*, *191*(1), 97-113.

Buscombe, D., & Masselink, G. (2006). Concepts in gravel beach dynamics. *Earth-Science Reviews*, *79*(1-2), 33-52.

Chabokpour, J., & Samadi, A. (2020). Analytical solution of reactive hybrid cells in series (HCIS) model for pollution transport through the rivers. *Hydrological sciences journal*, *65*(14), 2499-2507.

Chabokpour, J., Shojaei, B., & Azamathulla, H. (2024). Numerical investigation of river bed forms on pollution dispersion. *LARHYSS Journal P-ISSN 1112-3680/E-ISSN 2521-9782*(59), 211-228.

Church, M. (2006). Bed material transport and the morphology of alluvial river channels. *Annu. Rev. Earth Planet. Sci.*, *34*(1), 325-354.

Church, M. (2010). Gravel-bed rivers. *Sediment cascades: An integrated approach*, 241-269.

Cienciala, P., & Hassan, M. A. (2013). Linking spatial patterns of bed surface texture, bed mobility, and channel hydraulics in a mountain stream to potential spawning substrate for small resident trout. *Geomorphology*, *197*, 96-107.

Dingle, E. H., Sinclair, H. D., Venditti, J. G., Attal, M., Kinnaird, T. C., Creed, M., Quick, L., Nittrouer, J. A., & Gautam, D. (2020). Sediment dynamics across gravel-sand transitions: Implications for river stability

and floodplain recycling. *Geology*, *48*(5), 468-472.

Garcia, C., Cohen, H., Reid, I., Rovira, A., Ubeda, X., & Laronne, J. B. (2007). Processes of initiation of motion leading to bedload transport in gravel-bed rivers. *Geophysical Research Letters*, *34*(6).

Gomez, B., & Church, M. (1989). An assessment of bed load sediment transport formulae for gravel bed rivers. *Water Resources Research*, *25*(6), 1161-1186.

Gray, J. R., Laronne, J. B., & Marr, J. D. (2010). *Bedload-surrogate monitoring technologies* (2328-0328).

Hassan, M. A., Li, W., Viparelli, E., An, C., & Mitchell, A. J. (2023). Influence of sediment supply timing on bedload transport and bed surface texture during a single experimental hydrograph in gravel bed rivers. *Water Resources Research*, *59*(12), e2023WR035406.

Kadota, A., Suzuki, K., & Mori, K. (2001). Study on Flow Resistance Over Steep-Slope Gravel-Bed. *PROCEEDINGS OF HYDRAULIC ENGINEERING*, *45*, 619-624.

Konsoer, K. M., Rhoads, B. L., Langendoen, E. J., Best, J. L., Ursic, M. E., Abad, J. D., & Garcia, M. H. (2016). Spatial variability in bank resistance to erosion on a large meandering, mixed bedrock-alluvial river. *Geomorphology*, *252*, 80-97.

Lamarre, H., MacVicar, B., & Roy, A. G. (2005). Using passive integrated transponder (PIT) tags to investigate sediment transport in gravel-bed rivers. *Journal of Sedimentary Research*, *75*(4), 736-741.

Laronne, J. B., & Reid, L. (1993). Very high rates of bedload sediment transport by ephemeral desert rivers. *Nature*, *366*(6451), 148-150.

Marquis, G. A., & Roy, A. G. (2013). From macroturbulent flow structures to large-scale flow pulsations in gravel-bed rivers. *Coherent flow structures at Earth's surface*, 261-274.

Mosselman, E. (2012). Modelling sediment transport and morphodynamics of gravel-bed rivers. *Gravel-bed rivers: processes, tools, environments*, 101-115.

Mrokowska, M. M., & Rowiński, P. M. (2019). Impact of unsteady flow events on bedload transport: A review of laboratory experiments. *Water*, *11*(5), 907.

Palucis, M. C., Ulizio, T. P., Fuller, B., & Lamb, M. P. (2018). Flow resistance, sediment transport, and bedform development in a steep gravel-bedded river flume. *Geomorphology*, *320*, 111-126.

Papangelakis, E., & Hassan, M. A. (2016). The role of channel morphology on the mobility and dispersion of bed sediment in a small gravel-bed stream. *Earth Surface Processes and Landforms*, *41*(15), 2191-2206.

Parker, G., Fu, X., Lamb, M., & Venditti, J. (2020). Morphodynamics of downstream fining in rivers with unimodal sand-gravel feed.

Pfeiffer, A. M., Finnegan, N. J., & Willenbring, J. K. (2017). Sediment supply controls equilibrium channel geometry in gravel rivers. *Proceedings of the National Academy of Sciences*, *114*(13), 3346-3351.

Redolfi, M., Bertoldi, W., Tubino, M., & Welber, M. (2018). Bed load variability and morphology of gravel bed rivers subject to unsteady flow: A laboratory investigation. *Water Resources Research*, *54*(2), 842-862.

Robert, A. (2014). *River processes: an introduction to fluvial dynamics*. Routledge.

Roushangar, K., & Shahnazi, S. (2020). Prediction of sediment transport rates in gravel-bed rivers using Gaussian process regression. *Journal of hydroinformatics*, *22*(2), 249-262.

Singh, M., Singh, I. B., & Müller, G. (2007). Sediment characteristics and transportation dynamics of the Ganga River. *Geomorphology*, *86*(1-2), 144-175.

Wickert, A. D., & Schildgen, T. F. (2019). Long-profile evolution of transport-limited gravel-bed rivers. *Earth Surface Dynamics*, *7*(1), 17-43.

Wlodarczyk, K., Hassan, M. A., & Church, M. (2023). Annual and decadal net morphological displacement of a small gravel-bed channel. *Earth Surface Processes and Landforms*, *48*(8), 1630-1645.

Zhu, L. L., & Ge, H. (2014). Balance Adjustment of the gravel-sand river downstream reservoir. *Applied Mechanics and Materials*, *444*, 1218-1221.